ISBN: 978-3-95450-212-7 ISSN: 2673-5482 doi:10.18429/JACoW-CYCLOTRONS2022-MOPO001

# A REAL-TIME CONTROLLER FOR RAPID ENERGY DEGRADING OF THE CYCIAE-230 CYCLOTRON BEAM PRODUCTION SYSTEM*

Qiqi Song, Aolai He, Zhiguo Yin†, Tianyi Jiang, Hongru Cai, Bohan Zhao, Yang Wang, Qiankun Guo, Tianjue Zhang, China Institute of Atomic Energy, Beijing, China

*Abstract*

The energy selection system (ESS) plays an important role in a proton therapy system. Usually, it consists of an energy degrader, a set of achromatic bending magnets, an envelope collimator, and a momentum-selecting slit. In CIAE, a dedicated beam transportation line, including these essential elements, for the CYCIAE-230 superconducting cyclotron has been designed and manufactured for study purposes. To reduce the layer switching time, e.g. typically within 50 milliseconds, this ESS system takes advantage of VME-based real-time controller design. On one side, this controller uses S-curve to direct drive the step motors of various actuators, this is done by an off-the-shelf embedded controller. On the other hand, it uses Data Distribution Service (DDS) communication protocol to directly tap into the nozzle control system network. In such a manner, the energy requirement can be efficiently handled and the controller is also responsible for the current regulation for the 46 magnets. The design of this high-efficiency controller will be reported in this paper, both from hardware and software aspects. Preliminary test results will also be evaluated and analysed to direct further improvement of the system.

## INTRODUCTION

The rate of human suffering from tumours has been increasing in recent years [1], and proton therapy is one of the effective means to treat tumours. “Bragg peaks” occur during the energy release of proton rays, and the excellent dose distribution of this Bragg peak drives the energy of the proton beam to be released concentrated at cancer cells, so the location of the proton beam energy release is directly related to the proton beam energy, and the proton beam energy is adjusted to achieve radiotherapy at different depths in the tissue to kill cancer cells [2, 3]. In cyclotron-based proton therapy facilities, the energy variation of the proton beam is carried out by controlling the thickness of the degrader [4]. Currently, well-established degrader materials use graphite, boron carbide [5], and beryllium [6]. The CYCIAE-230 is designed to achieve beam energy control mainly by controlling the graphite degrader of the double-wedge shape. The energy selection system (ESS) usually consists of an energy degrader, a set of achromatic bending magnets, an envelope collimator, and a momentum-selecting slit. In CIAE, a dedicated beam transportation line, including these essential elements, for the CYCIAE-230 superconducting cyclotron has been designed and manufactured for study purposes.

* Work supported by Zhiguo Yin
† zhiguoyin@ciae.ac.cn

## OVERVIEW OF THE REAL-TIME CONTROL SYSTEM

The real-time control system (Fig. 1) is divided into a hardware part and a software part. The hardware part includes the VxWorks-based VME bus controller, while the software part is developed based on Qt and communicates between devices via the DDS middleware protocol. This real time controller is highly reliable and real time, and is able to quickly control the devices on the ESS section to adjust them to the appropriate values, it is capable of controlling the beam energy from 70 MeV to 240 MeV. The control effect of the controller is mainly reflected in: adjusting the degrader to the corresponding thickness to control the beam energy; adjusting the envelope collimator and the energy-selective slit to the corresponding position for suppressing the growth of beam emissivity; and indicating the achromatic bending magnets to the corresponding value to control the trajectory of the beam motion.

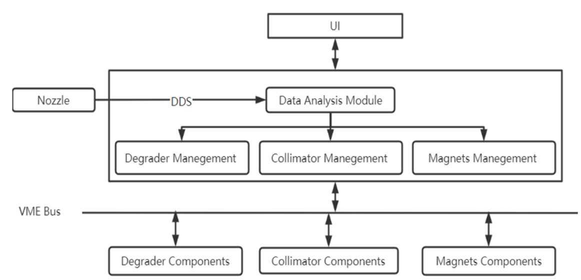


Figure 1: Architecture of the real-time control system.

Table 1: Performance Comparison of Existing Energy Degraders

| Manufacturer | Energy range | Material | Shape | Energy switching time |
|---|---|---|---|---|
| IBA | 70~230 MeV | C | Spiral type | ≈ 500ms |
| Varian | 70~250 MeV | C | Triangular wedge | ≈ 150ms |
| Pronova | 70~230 MeV | Be | Double-wedge wing type | ≈ 500ms |

Compared with the existing well-known degraders, as in Table 1, the real-time control system is able to receive energy information and issue commands to adjust the degrader to the corresponding energy position within 50 ms.

Content from this work may be used under the terms of the CC-BY-4.0 licence (© 2022). Any distribution of this work must maintain attribution to the author(s), title of the work, publisher, and DOI

ISBN: 978-3-95450-212-7 ISSN: 2673-5482 doi:10.18429/JACoW-CYCLOTRONS2022-MOPO001

## HARDWARE COMPONENTS OF THE REAL-TIME CONTROLLER

The hardware part (Fig. 2) uses the MVME6100 VME single board computer as, which provides the VxWorks board support package. The stepper motor control is implemented by a MAXv motion controller, which can control up to 8 axes of the stepper system.

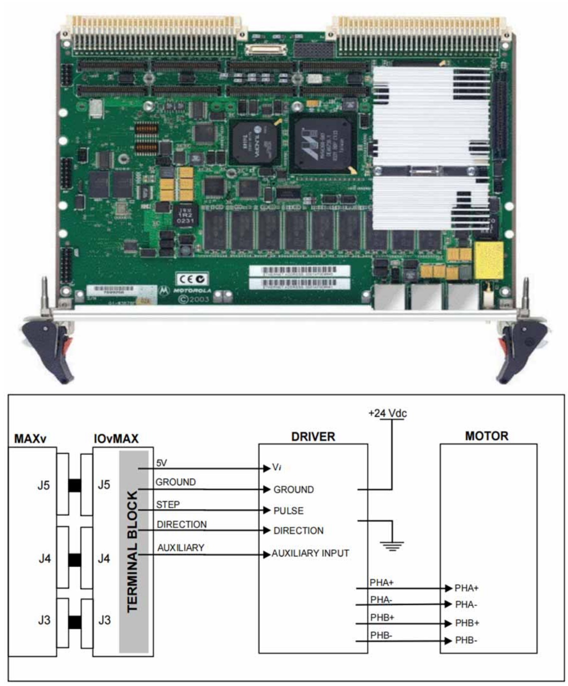

Figure 2: Hardware components for real-time controller, a) system board MVME6100, b) wiring diagram of MAXv controller via the IOvMAX interface module.

On the MVME6100, data is exchanged with each module through the VME backplane bus to control each processing module and display the signal processing results. The MVME6100 module runs under the embedded real-time operating system VxWorks. The MVME6100 provides a network interface that enables the system to communicate with the controllers of the achromatic bending magnets through this network interface, instructing them to adjust the current and PID to the appropriate values.

Self-developed signal transmission combinations (Fig. 3) are used to isolate motion controllers, reduce neutron interference near the beam line, and improve the reliability of data transmission.

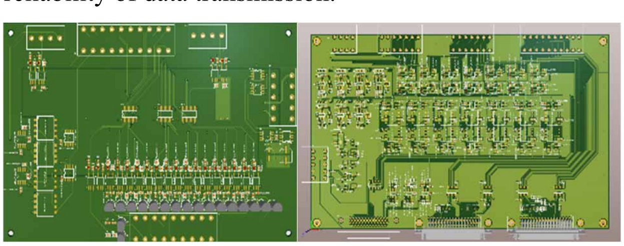
Figure 3: Signal transmission combinations, a) motor signal board, b) position signal board.

## SOFTWARE OF THE REAL-TIME CONTROLLER

### *Software Architecture*

The software of this real-time controller is deployed in the VxWorks real-time control system and is divided into three parts: DDS communication, real-time task calling, and data processing. The software system uses DDS communication as the main task and designs a unique subtask scheduling sequence based on the characteristics of the VxWorks operating system, which includes the control of different devices under the ESS as several different subtasks.

### *Database Preparation*

The main function of the energy degrader is to realize the energy drop using the Bethe-Bloch formula shown in Eq. (1):

$$-\left(\frac{dE}{dx}\right) = 4\pi N_a r_e^2 m_e c^2 z^2 \cdot \left(\frac{Z}{A}\right)\left(\frac{1}{\beta^2}\right)\left[\ln\left(\frac{2m_e c^2\gamma^2\beta^2}{I}\right) - \beta^2 - \frac{\delta}{2}\right] \quad (1)$$

where $E$ denotes the particle energy, $x = X \cdot \rho$ is the thickness of the medium, $r_e$ is the classical electron radius, $m_e$ is the electronrest mass, $c$ is the speed of light, $z$ is the amount of particle variation, $\frac{Z}{A}$ is the specific charge of the energy-reducing material, $\beta, \gamma$ is the relativistic factor, $I$ is the ionization potential, and $\frac{\delta}{2}$ denotes the density effect.

In addition to the energy loss, the proton beam passing through the degrader target material also collides with atomic nuclei, resulting in multiple Coulomb scattering effects and causing an increase in the beam geometric emittance. The emissivity of the beam passing through the degrader is shown in Eq. (2):

$$\varepsilon_1 = \varepsilon_0 + \langle\theta_x^2\rangle \sum_i \beta_i \quad (2)$$

where $\varepsilon_0$ and $\varepsilon_1$ are the beam emissivity before and after the beam passes through the degrader, respectively, and $\langle\theta_x^2\rangle$ is the mean square value of the emissivity growth versus the multiple scattering angle after the beam passes through the degrader; $\beta$ is the TWISS parameter characterizing the size of the beam envelope.

According to the range of the beam in every 2 mm of water, this project has been converted to obtain the range of the beam in graphite as the thickness of the energy-reducing material corresponding to each energy layer. CYCIAE-230 calculates the thickness of the degraded material at the specified arrival beam energy by SRIM and stores it in the database.

The energy range of proton therapy is 70 MeV to 240 MeV, which is a wide energy range and a set of PID parameters is difficult to adapt to all the full energy range. For the three deflection magnets of CYCIAE-230, three different sets of PID parameters are used in the beam

Content from this work may be used under the terms of the CC-BY-4.0 licence (© 2022). Any distribution of this work must maintain attribution to the author(s), title of the work, publisher, and DOI

ISBN: 978-3-95450-212-7 ISSN: 2673-5482 doi:10.18429/JACoW-CYCLOTRONS2022-MOPO001

energy range between 240 MeV and 145 MeV, 145 MeV and 110 MeV, 110 MeV and 70 MeV, separately. The controller passes the corresponding PID parameters for different energy bands to the magnet controller by calling the SQL database.

### *Communication Advantage*

In order to receive energy information from the nozzle in real time, the controller communicates with the nozzle via the Data Distribution Services (DDS) bus. As a subscriber of information, this real-time controller can quickly acquire data and process it while the nozzle is releasing energy information (Fig. 4), which has the advantage of reducing the communication time between systems.

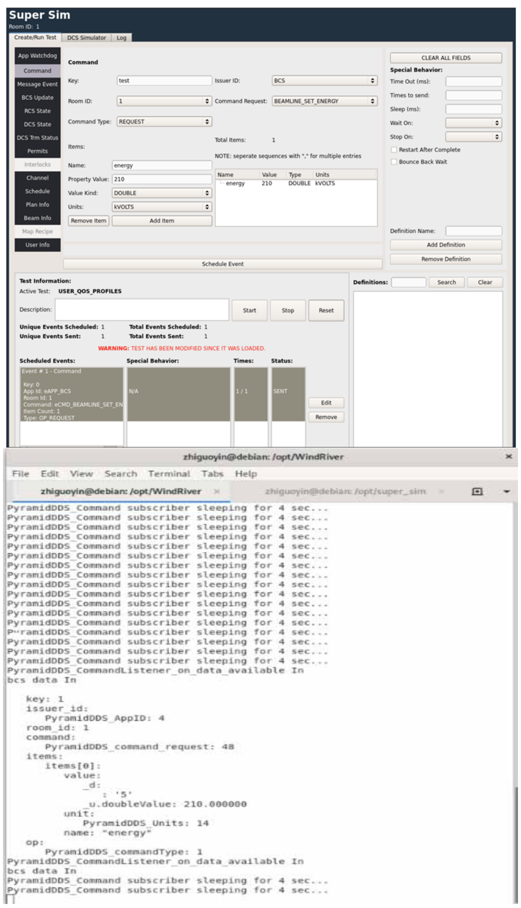

Figure 4: Controller communicates with Nozzle via DDS, a) the nozzle simulator sends energy messages, b) The controller receives beam energy information.

Open-loop control of the magnet power supply is achieved by real-time monitoring of the current, voltage, and component status of the 43 magnet power supplies (see Fig. 5).

The real-time controller interacts with the achromatic bending magnet powers based on the UDP protocol. This communication method is simple and fast, and its communication time is in the nanosecond range.

Figure 5: Open-loop control of ESS magnet power supply

### *S-Curve Algorithm of Motion Controller*

The control of the stepper motor is realized by the motion controller, which uses an S-curve algorithm to regulate the speed of the stepper motor. Since the torque of the stepper motor may not be able to drive the load, this can result in the stepper motor not turning as many degrees as the number of degrees corresponding to the input pulse.

The graphite degrader used in CYCIAE-230 requires a certain thickness for the wedge structure to meet the energy reducing conditions, so the unavoidable problem is that the stepper motor needs to drive a large mass of degrader material.

By setting the optimal parameters of the S-Curve algorithm (Fig. 6) in the software system of the real-time controller, the stepper motor is able to adjust its speed to the specified value in a smooth and fast manner, thus avoiding the motor "out-of-step" phenomenon and reducing the negative effects of possible damage to the stepper motor due to the high inertia of the controlled device.

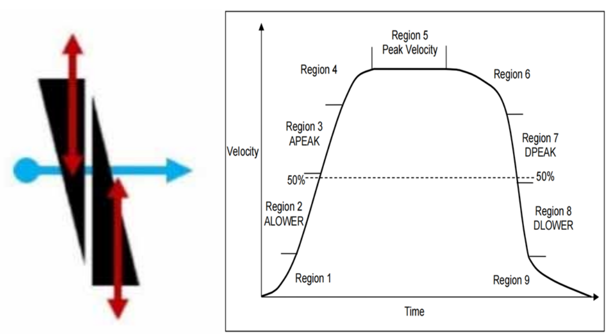


Figure 6: Motion design by S-curve algorithm, a) the graphite degrader, b) S-Curve algorithm.

## TEST RESULTS AND FUTURE WORK

CYCIAE-230 has now completed the equipment installation and commissioning of the ESS section: including the energy degrader installation, the envelope collimator installation, the achromatic bending magnet power performance test, and the real-time controller performance test.

The results of the current tests show that the real-time controller receives energy from the nozzle at each level of energy switching, and is able to control the energy degrader, a set of achromatic bending magnets, the envelope collimator, and the momentum-selecting slit to move or adjust these devices to a specified position or value within 50 ms (Fig. 7).



Content from this work may be used under the terms of the CC-BY-4.0 licence (© 2022). Any distribution of this work must maintain attribution to the author(s), title of the work, publisher, and DOI

ISBN: 978-3-95450-212-7 ISSN: 2673-5482 doi:10.18429/JACoW-CYCLOTRONS2022-MOP0001

Content from this work may be used under the terms of the CC-BY-4.0 licence (© 2022). Any distribution of this work must maintain attribution to the author(s), title of the work, publisher, and DOI

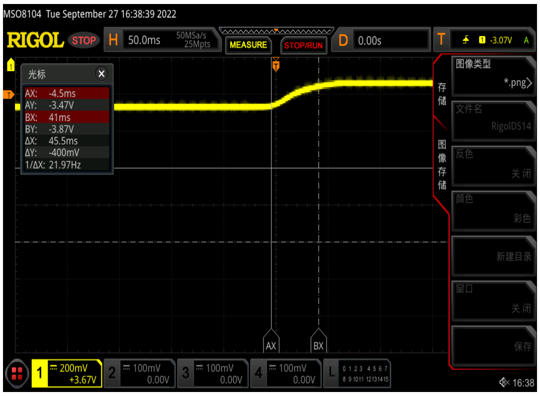

Figure 7: Energy degrader response time.

With the detection results of the position information returned at the device, the accuracy is up to 0.1%.

In 2023, the energy selection system will be tested under real beam conditions, and the reliability of the real-time controller will be further determined by combining numerical analysis of the magnetic properties with a more accurate determination of the actual response time in the real-time controller.

## REFERENCES

[1] F. Bray *et al.*, "Global cancer statistics 2018: GLOBOCAN estimates of incidence and mortality worldwide for 36 cancers in 185 countries," *CA Cancer J. Clin.*, vol. 70, no. 4, p. 313, Nov. 2018. doi:10.3322/caac.21492

[2] T. Zhang *et al.*, "Developments for 230 MeV Superconducting Cyclotrons for Proton Therapy and Proton Irradiation," *Nucl. Instrum. Methods Phys. Res. Sect. B*, vol. 406, part A, pp. 244-249, Sept. 2017. doi:10.1016/j-nimb.2016.11.010

[3] R. R. Wilson, "Radiological use of fast protons," *Radiology*, vol. 47, no. 5, p. 487, Nov. 1946. doi:10.1148/47.5.487

[4] V. Rizzoglio *et al.*, "On the accuracy of Monte Carlo based beam dynamics models for the degrader in proton therapy facilities," *Nucl. Instrum. Methods Phys. Res. Sect. A*, vol. 898, pp. 1-10, Aug. 2018. doi:10.1016/j.nima.2018.04.057

[5] C. M. Charlie Ma, T. Lomax, *Proton and Carbon Ion Therapy*, CRC Press, Taylor & Francis Group, 2013.

[6] V. A. Anferov, "Energy degrader optimization for medical beam lines," *Nucl. Instrum. Methods Phys. Res. Sect. A*, vol. 496, no. 1, pp. 222-227, Jan. 2003. doi:10.1016/S0168-9002(02)01625-X